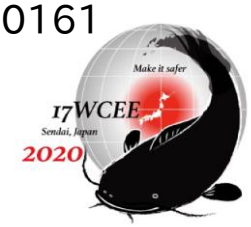

17th World Conference on Earthquake Engineering, 17WCEE
Sendai, Japan - September 13th to 18th 2020

DUCTILITY QUANTIFICATION IN SCBF SYSTEM WITH DIFFERENT END CONNECTIONS: AN EXPERIMENTAL STUDY

P. Patra[(1)], D.R. Sahoo[(2)], A.K. Jain[(3)]

[(1)] *PhD Scholar, Indian Institute of Technology Delhi, pratikpatra5@gmail.com*
[(2)] *Associate Professor, Indian Institute of Technology Delhi, drsahoo@civil.iitd.ac.in*
[(3)] *Professor, Indian Institute of Technology Delhi, akjain@civil.iitd.ac.in*

Abstract

Special concentrically braced frames (SCBFs) are considered as the most effective lateral force-resisting systems in building structures. The ease of the construction and accessibility made the braces most attractive fuse element in the earthquake-prone area. In recent studies, it was found that new type of connections is being introduced to enhance the ductility of the braced frame system. Past earthquake and experimental studies show that the connections are more prone to failure in the braced frame system. In the present study, three large scale experiments were conducted on the three types of end connection based on the hinge location and orientation of the plate, namely, a) out-of-plane buckling (OOPB) braced system b) in-plane buckling (IPB) braced system and c) Direct connection (DC) braced system. The critical limit states based on the type of the connection were discussed and design method was proposed in the study to prevent premature failure. The performance of the braced system was quantified based on the hysteric response, displacement ductility and post-buckling strength. It is found that the flexibility of the end hinges has direct influence on the performance of the brace-connection sub-assemblage system. Lower stiffness of the end hinges of OOPB braced system lead to best performance among all the connection. DC braced system performance is almost similar to that of IPB brace system, but the former observed to enhance its displacement ductility by accumulating plastic strain at end hinges. The sequence of the damage states is observed in the specimens are discussed. It is also found that the post-buckling strength reduces with the increase in the flexibility of the end hinges.

Keywords: Fracture, in-plane buckling, post-buckling strength, critical limits states, knife plate

1. Introduction

One of the mostly used passive lateral load resistance system in the earthquake-prone areas are concentrically braced frame system (CBFs). Easy fabrication, availability of material and higher strength to weight ratio attract many designers to opt for the concentrically braced frame system in the highly seismic region. Special concentrically braced frames (SCBFs) are the type of CBFs designed for the high level of ductility and energy dissipation [1–3]. In the SCBFs system, the hysteretic energy is dissipated through the formation of plastic hinges in the brace element as well as brace-connection assembly. The plastic hinge at the middle of the brace is called as the primary hinge, which is mostly responsible for the energy dissipation [4,5]. The location of the other two hinges are based on the design of the end connection. Fig. 1 shows the various type of end connections based on the location of the secondary hinges or end hinges. These end connections are called as out-of-plane buckling braced system (OOPB), in-plane buckling braced system (IPB), and direct connection braced system (DC). IPB brace system was newly developed connection arrangement to prevent damage of the non-structural components by forcing the brace to buckle in the plane of the braced frame [6,7]. This also helps to decrease the post-recovery time and a small step toward a resilient structure.

AISC 341-16 [8] mostly uses OOPB brace system for the SCBF structures. AISC 341-16 [8] has introduced for the first time the IPB brace system. AIJ 2012 [9] use the DC brace system in CBFs. In this case, braces used are mostly made of open steel sections, in which the end section can provide enough strength to the beam-column-brace connection. DC braced system provide the higher buckling strength because of the low effective length factor. However, past studies on the influence of such connections on the displacement ductility of braced frames are very limited.

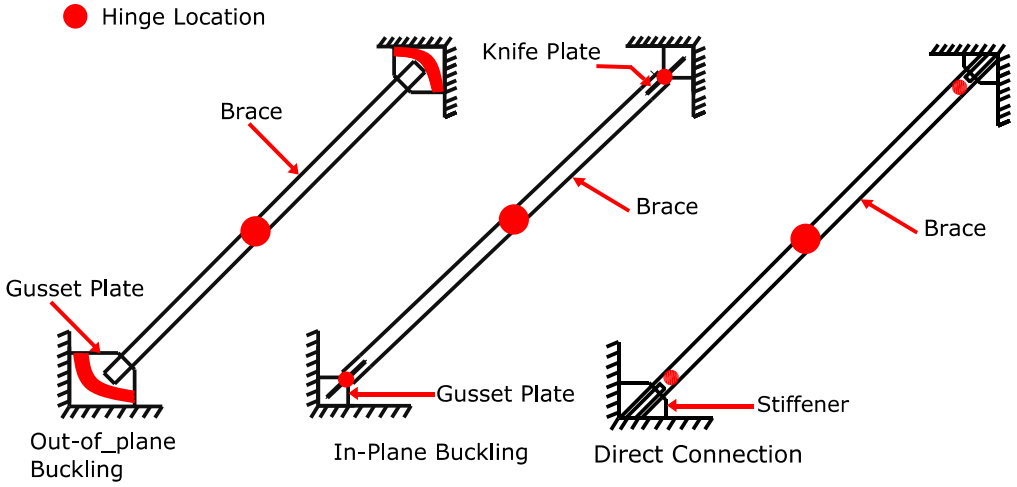

Fig. 1 – Different types of connections in SCBF.

This study is focused on the evaluation of cyclic performance of large-scale braces with three types of end connections. Reversed-cyclic displacement control quasi-static tests have been conducted to quantify the influence of the end connection on the ductility of the braced frame structures. Hollow circular sections were used as brace section in all the three tests. All the parameters are kept constant except the end connection detailing, in order to get a direct comparison of different types of connection. The behavior of these specimens has been compared based on the flexibility of end connections, the sequence of the damage states, and the magnitude of story drift and axial strain in braces. Critical limit states for the connection are highlighted and the proposed design procedure was discussed to avoid premature failure. For the OOPB brace system, three different interface weld criteria are compared, and the economical weld design criteria have been proposed.

For the IPB brace system, limit states such as interface weld of the gusset plate and out-of-plane bending of the gusset plate are discussed. For the DC brace system, end connection design procedure has been proposed such that pre-mature fracture can be avoided, and the location of the end hinges can be pre-defined. The parameters studied are hysteretic response, post-buckling strength, damage states and displacement ductility. Based on the experimental results, the trend of behavior was established and quantification in term of flexibility of the end connection was discussed.

2. Critical Limit States

Past studies have shown premature failure of the connection of the SCBFs system. Different connection required different limit states to be checked to avoid premature failure and to have desire yield hierarchy. The design of the connection has evolved a lot through the research conducted in the last two decades. This section discusses the critical limit states that were mostly absent in the past studies, and economical interface weld size for the OOPB braced system.

2.1 OOPB Braced System

Most of the past studies have focused on the design, detailing and performance of OOPB SCBF system. In the present study, rectangular gusset plate with $8t_p$ (t_p is the thickness of the gusset plate) elliptical clearance end connection was used for the experimental investigation. One of the most critical limit states for the OOPB brace system is the interface weld of the gusset plate. Three different procedures are provided in the literature to calculate the size of the interface weld [8,10]. These methods are 1) interface weld size based on balanced design procedure 2) maximum shear strength of the gusset plate and 3) maximum weak-axis flexural strength of gusset plate. A detail discussion of these limit states can be found elsewhere [11].

The weld size calculated based on the balanced design procedure and maximum shear strength of the gusset plate consumed 178% and 125% more volume of weld material for the bottom gusset plate and 56% and 27% more volume of weld material for the top gusset plate respectively. No large-scale experiments have been conducted till date conducted to evaluate the performance of the weld designed based of the concepts of weak-axis flexure strength of gusset plate despite the fact that it provides the lowest size of the weld. The interface weld of the gusset plate to the beam-column junction for the OOPB specimen that was tested in the study, was calculated based on the concept of weak-axis flexural strength. The interface forces calculated from Uniform force method (UFM) and Generalized uniform force method (GUFM) provide almost similar weld sized for the connection of the gusset plate and beam-column junction.

2.2 IPB Braced System

The damage of the non-structural components due to out-of-plane buckling of the braced specimen are shown in the past earthquakes. To prevent such failure, an innovative in-plane buckling brace system was first proposed by Lumpkin 2009 [6] with $2t_p$ linear clearance. Later Tsai 2013 [12] modified it with $3t_p$ linear clearance which has been included in the AISC 341-16 [8]. Recent tests conducted by sen *et. al.* [13] and Tsai *et. al.* [12], showed some critical failure modes for the IPB brace system, such as, out-of-plane bending of the gusset plate, failure of interface weld size and tearing of knife plate [Fig. 2(a), (b) and (c)]. In the present study, the possible instabilities have been controlled such that desire yield hierarchy and brace fracture at the middle of the brace could be achieved. Three most critical modes of failure were taken into consideration for the design. The interface weld of the gusset plate was expected to subjected a force demand different than that of the OOPB brace system because the gusset plate of IPB braced system were designed to remain elastic. The author proposed a design method to calculate the interface weld based on the bending of the knife plate and weak-axis flexural strength of the gusset plate. IBP braced system can be ineffective if the brace buckles in out-of-plane. To prevent such critical limit state, a method has been proposed to calculate the out-of-plane buckling strength of the IPB brace system through the gusset plate. The yield line in the gusset plate was chosen such that it provides least resistance to buckling. The criteria to prevent buckling was set based on the law that a physical phenomenon follows a path that required least resistance. The detail formula for the above two limit states proposed by the author can be found elsewhere [11,14]. To prevent tearing of the knife plate,

the demand on the knife plate was checked with the bending capacity of the knife plate along with the axial force of the brace member.

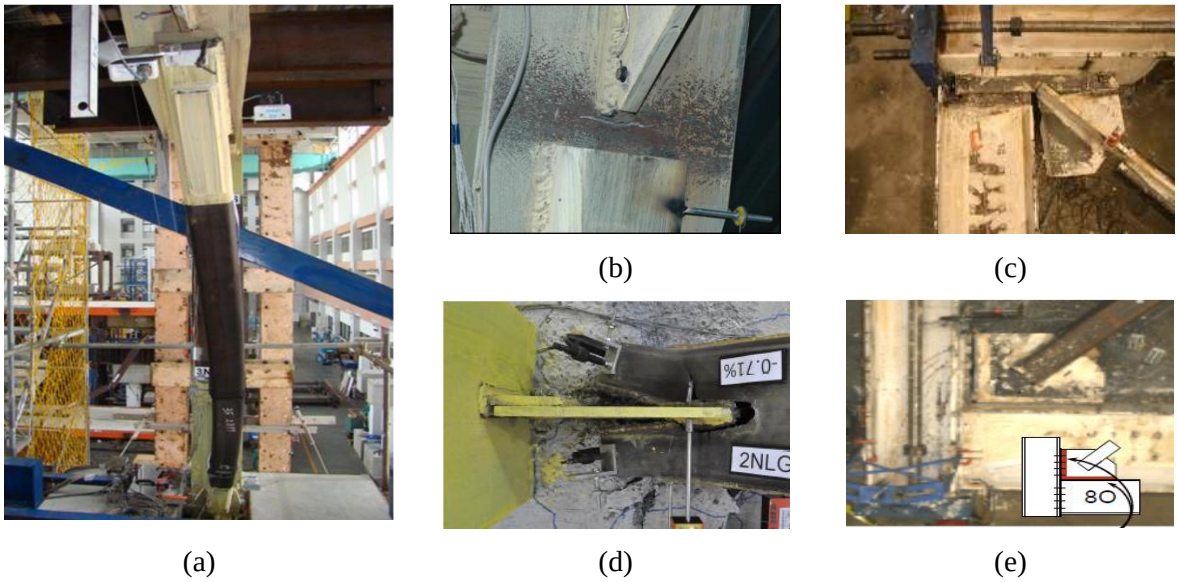

(a) (b) (c) (d) (e)

Fig 2. Failure modes observed in IPB and DC braced system

2.3 DC Braced System

Fig. 2(d) and (e) shows the mode of failure observed for the DC braced system with hollow structural section. The demand for these connections are very high and depend on the flexural capacity of the brace specimen. The sections used for the connection generally does not provide enough strength to withstand the demand. The location of the end hinges is also not clearly defined for the DC braced system. In order to avoid end connection failure of the DC braced system, in the present study, stiffener plate has been used to withstand the demand on the end connection due to the flexural capacity of the brace. In order to ensure the formation of end hinges at particular locations, the use of reinforcement plates has been proposed. The sizes of the stiffener plate have been calculated based on the flexural capacity of the brace section about the two critical buckling direction. The reinforcement plate having area about 30% of the brace section has been used on both sides of the stiffener plate. The reinforcement plate is extended toward the end of the end connection and welded at the beam-column junction. The reinforcement plate is also extended 60mm toward the middle of the brace such that failure at the stiffener plate end can be avoided and hinge location can be shifted to prescribe location. Here, the location for the end hinges has been decided to form at end of the reinforcement plates.

3. Experimental Program

Three large-scale tests were conducted in the Heavy Structural laboratory of IIT Delhi on hollow circular section steel braces. Displacement control quasi-static cyclic loading was applied to the specimens up to the fracture. The test set up used in the experiment is shown in Fig 3. The instrumentation used to capture different behavior of the brace system is shown in Fig. 4.

Hollow circular sections HCS 76.1x2.9 were used as brace members. OOPB specimen was designed and detailed for the out-of-plane buckling with rectangular section gusset plate and $8t_p$ elliptical clearance. IPB specimen was designed and detailed for the in-plane buckling with $3t_p$ linear clearance. IPB specimen was consisted of gusset plate, knife plate and brace section. Knife plate was responsible for the in-plane buckling of brace. DC specimen was detailed such that all the hinges would form in the braces. The design procedure and limits states discussed earlier were used in the design and detailing of the test specimens. Table 1 highlighted the detail of the tested specimen. The brace angle used in the testing was 45°. The length of the brace was taken as the end to end length of brace member. For the DC specimen, the length of brace was taken

as the free length after the reinforcement plates. The slenderness ratio of the test specimens has chosen in such a way that it would resemble a real structure. Coupon tests were conducted to measure the material properties of the brace section and the plate. Table 2 shows the measured material properties of the member tested. Fig. 5 shows the cyclic loading protocol used for the experimental investigation.

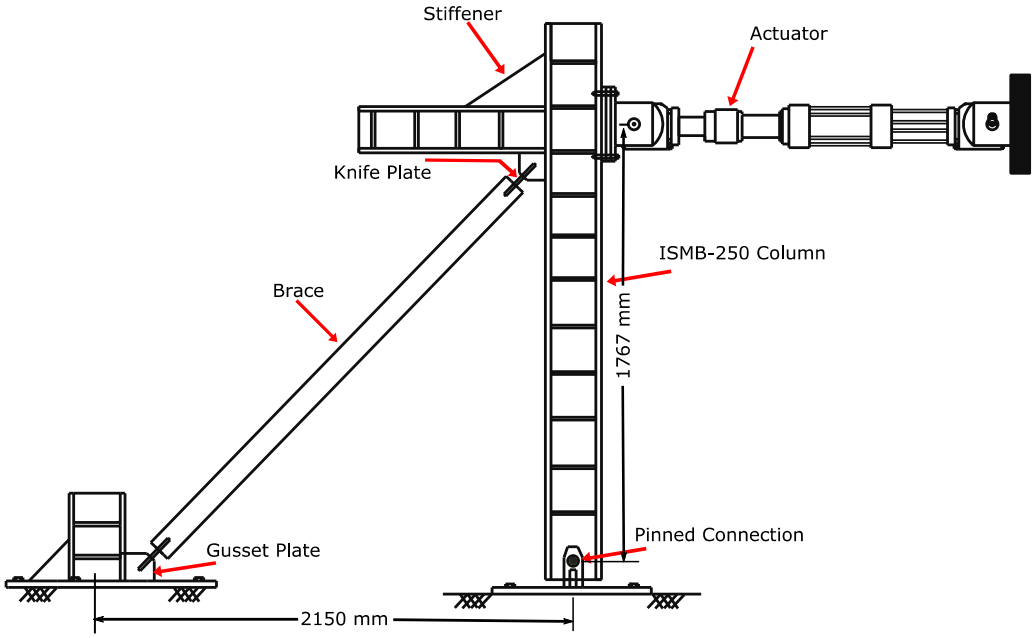

Fig. 3 - Test setup used in the Experiment

4. Hysteretic Response

Fig 5 shows the hysteretic response of the OOPB, IPB and DC specimens respectively. All the specimen goes through different modes at different axial strain. The mode of failure observed in all test specimens was the fracture of braces at their mid-lengths without any instability. The buckling strengths of the brace specimen OOPB, IPB and DC were noted as 129.4 kN, 142.3 kN and 166.6 kN, respectively. The variation in the buckling loads was primarily due to the difference in the bending stiffness that is associated with end hinges of the brace-connection assembly. The range of story drift observed for the OOPB, IPB and DC specimen were 5.2%, 3.8% and 3.4% respectively.

The change in the performance was only attributed to the end connections of the specimen as all other parameters are kept constant. Table 3 shows the stiffness and the plastic moment of the end hinges. The stiffness of the end hinges for the OOPB specimen for the top and bottom gusset plate are 9.6 kN/m and 5.7 kN/m, respectively. For the IPB specimen, its value for the knife plate was 39.6 kN/m. Because of the high stiffness of the end connection of IPB specimen, OOPB specimen showed the higher story drift capacity. In case of the DC specimen, the end hinges were formed in the braces, which had the moment capacity of about 4.11 kNm. This resulted in the smaller story drift of the DC specimen as compared to the OOPB specimen and IPB specimen.

Fig. 5(d) shows the displacement ductility of the tested brace specimen. OOPB shows the highest displacement ductility followed by the IPB and DC specimen. DC and IPB specimen showed almost similar displacement ductility. It is generally expected that DC specimen would exhibit the lowest ductility as all plastic hinges are expected to form in the braces. This may increase the accumulation of the plastic strain in the middle of the brace leading to the early fracture. However, test results showed almost the opposite behavior. From the damage modes, it was observed that the end hinges of the DC specimen was bulged out, which helped in the accumulation of the plastic strain at the end. Hence, this reduced the rate of accumulation of the plastic

strain at middle of the brace section and enhanced the ductility of the brace system. This shows that hollow structural section having DC type end connection may enhance the ductility by accumulating the plastic strain at the end hinges. This kind of behavior may not be expected in the open section braces reducing their displacement ductility.

Fig. 4 - Detail of test setup and instrumentation

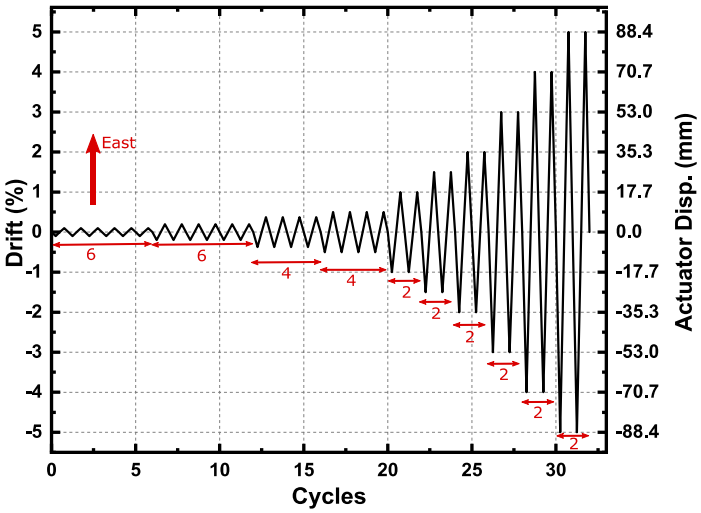

Fig. 5. Cyclic loading protocol for the tested specimens

Table 1. Detail of test specimens

Specimen	Section	Length	K	Slenderness ratio ($\lambda_{Spec.}$)	Compactness ratio $(D/t)_{Spec.}$	Theta (θ)
OOPB	HCS 76.1x2.9	2175	1	84	25.9	45
IPB-1	HCS 76.1x2.9	2160	1	83	25.9	45
DC	HCS 76.1x2.9	*2052	0.5	49	25.9	45

*Free length after the reinforcement plates

Table-2. Measured material properties

Section	Material grade	Yield stress (MPa)	Ultimate stress (MPa)	(R_y)
HCS 76.1x2.9	YSt210	284	373	1.35
Plate (6 mm thickness)	E 250	308	470	1.23
Plate (8 mm thickness)	E 250	313	481	1.25

R_y = ratio of the expected yield stress to the specified minimum/nominal yield stress

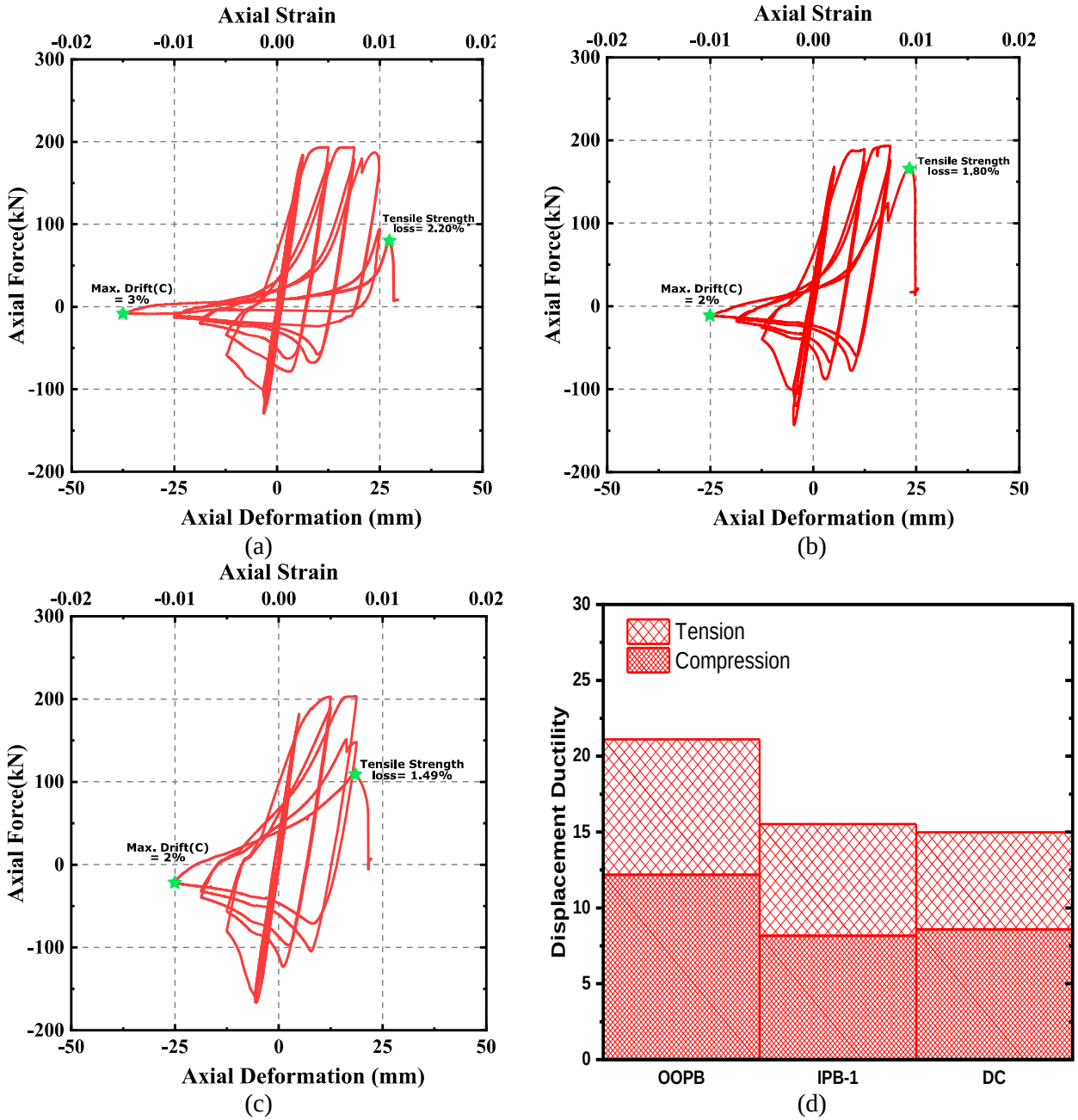

Fig 6. Hysteretic Response a) OOPB specimen b) IPB specimen c) DC specimen (d) Displacment ductility

Table 3 – Properties of the end hinges

Specimen	Whitmore width	L_{eff}	$K = \frac{EI_g}{L_{eff}}$,kN/m	$M_P = 1.1R_y f_y Z_p$ (kNm)
OOPB	214.7	80.50[a],136.54[b]	9.6[a] ,5.7[b]	0.60[a] ,0.60[b]
IPB-1	220	20	39.6	0.62
DC	-	-	-	4.11

[a] Top gusset Plate [b] Bottom gusset plate

5. Damage patterns and Modes of failure

In this section, summary of the various damage modes observed during the experiments are discussed. The concentrically brace specimen goes through different damage states before the final loss of strength. Table 4 listed different damage states the brace section and its connection undergoes before failure. It also highlights the story drift, loading drift, cycle number and its position in the loading cycle. Fig. 7 states some of the damage states observed during the experiments. The flake of whitewash was noted after the ample amount of whitewash peel off from the section. The story drift that lead to local buckling stages such as bulging and cupping [Fig. 7 (b) and (c)] were noted during the test. All the specimens went through the damage states but at different drift level despite being the same brace section and loading sequence. This section highlighted the influence of the connection on the different states observed during the experiments.

Table 4. Observation of damage states during the test

Drift (%)	Cycle drift(%) (Cycle no.)	Position and direction of loading	Damage states
Specimen OOPB			
0.26	0.375(1st)	Comp. & peak	Global Buckling
0.62	1(1st)	Comp. & loading	Flake of whitewash near the middle of brace
1	1(1st)	Comp. & loading	Flake of whitewash at top gusset plate
1	1(2nd)	Comp. & Peak	Local blugging near middle of the brace
1.5	1.5(1st)	Comp. & Peak	Flake of whitewash at bottom of gusset plate
1.44	2(1st)	Tension & loading	Initiation of fracture on front face near middle of brace
1.60	2(1st)	Tension & loading	Tearing across the section of brace
2.20	3(1st)	Tension & loading	Fracture near the middle of brace
Specimen IPB			
0.36	0.375(1st)	Comp. & peak	Global Buckling
0.54	1(1st)	Comp. & loading	Flake of whitewash at mid location of brace
0.75	1(1st)	Comp. & loading	Flake of whitewash at top and bottom of knife plate
1	1(1st)	Comp. & Peak	Local cupping at the middle of brace section
1.26	2(1st)	Tension & loading	Tearing across the section of brace
1.80	2(1st)	Tension & loading	Fracture at middle of brace
Specimen DC			
0.36	0.375(1st)	Comp. & peak	Global buckling
0.58	1(1st)	Comp. & loading	Flake of whitewash near middle of brace and at top a bottom connection at the end of the reinforcement pla local bugging near middle of brace
1.5	1.5(1st)	Comp. & peak	Blugging of brace at both end
1.5	1.5(1st)	Tension & peak	Initiation of crack on top face near middle of brace
1.36	1.5(1st)	Tension & loading	Tearing across the section of brace
1.49	2(1st)	Tension & loading	Fracture near the middle of brace

Comp.- loading toward the compressive side, Tension- loading toward the tension side, Peak- the point in the hysteresis graph where slope is zero, loading- when the load moves from zero drift toward the tensile or compressive cycle.

The flaking of whitewash was observed during the formation of the local buckling at the brace section in all the test specimen and propagated towards the connection when the cyclic drift increased. However, the observed length of the flake of whitewash differed in the type of specimens tested. It was found that, the specimen with the higher drift ratio has the higher span of spread of uncoated whitewash and vice-versa. Similarly, the tendency of formation of local buckling varied across the specimen and delayed to higher story drift for the specimen that has achieved the higher fracture ductility. The sequence of flake of whitewash and the local buckling are followed as: OOPB>IPB>DC. The smaller flexibility of the connection resulted in the higher the performance of the brace frame system.

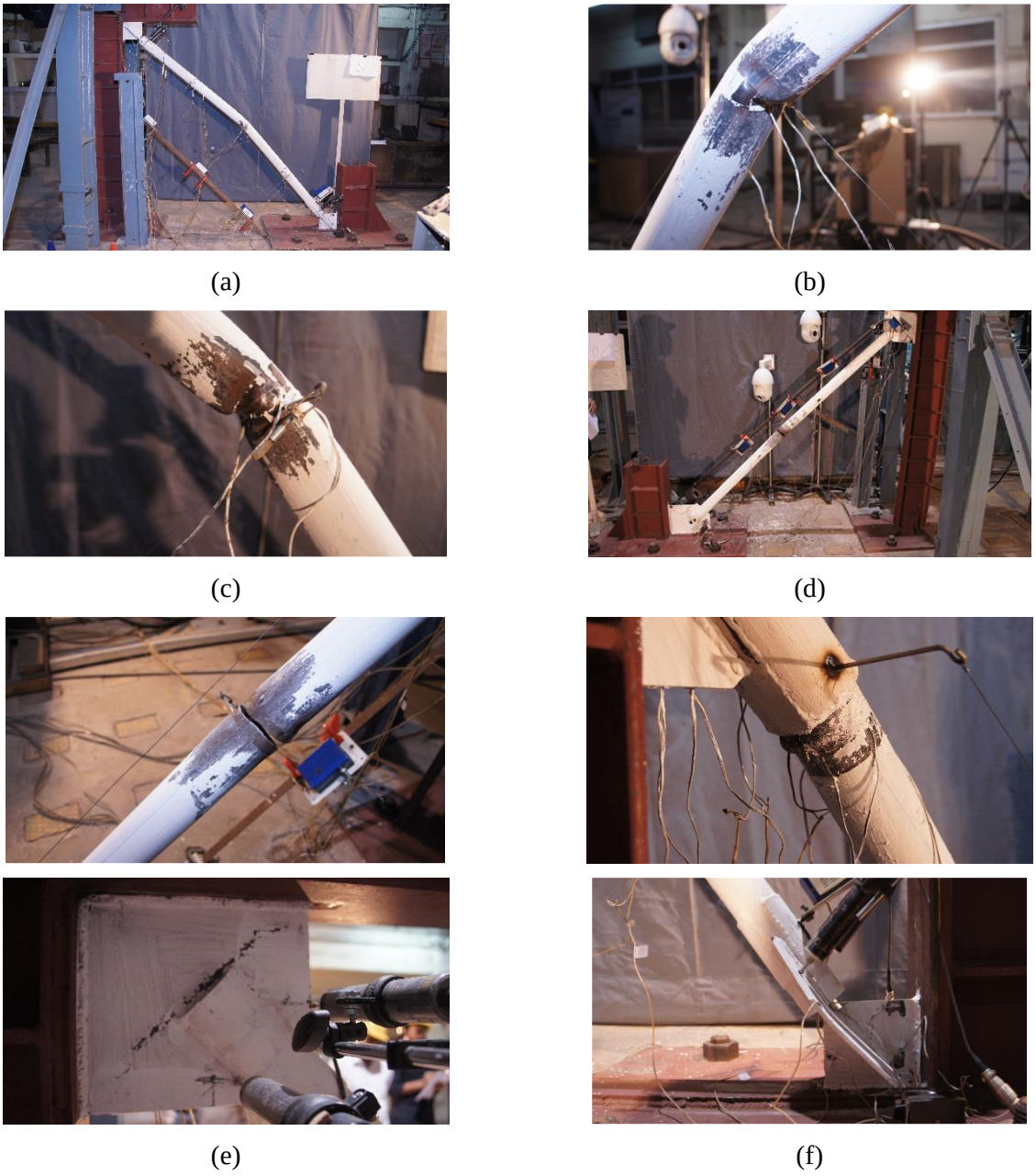

Fig. 7 Different damage states for the brace specimen observed during the experiments.

All the connections of test specimens were designed to withstand the expected strengths of the brace section. In the OOPB specimen, the flaking of whitewash started at the intersection of the free edge and restrained edge and propagated towards the end of the gusset plate-brace connection. But, in case of IPB specimens, the start of the flaking of whitewash was observed at center of knife plate and propagated towards the free edges. This was due to the free edges of the knife plates providing smaller restraint to bending as compared to the two perpendicular welded edge of the gusset plate. This prevented free bending and the similar trend was observed in the past study [15]. The sequence of damage in the end hinge plate observed during the experiments was follows: IPB<top gusset of OOPB<bottom gusset of OOPB.

Specimen IPB-1 has shown early flaking of whitewash because of the lower flexibility due to lower linear clearance. The top and bottom gusset plate showed two different lateral drifts corresponding to the initiation of yielding/damage. This is due to the difference aspect ratio between top gusset plate (1.1) and

bottom gusset plate (1.3). Thus, the higher aspect ratio of gusset plates results in the higher the flexibility and higher lateral drift corresponding to the initiation damages.

6. Influence of End Connections on Design Parameters

Premature failure of brace-connection sub-assemblage system can lead to the accumulation of the story drift at a particular story of the braced frame structure, resulting in the soft story mechanism. During the analysis, the fracture ductility of the braces is required to assess the performance of the braced frame. Table 7 shows the comparison of experimental displacement ductility with the ASCE 41-17 [16]. Displacement ductility is calculated as the ratio of the total axial displacement to the yield displacement of the components. The error percentage is calculated based on difference of the code prescribed value to the experimentally observed value. The positive error means unconservative brace member behavior which may lead to the soft story mechanism. It is found that ductility predicted by AISC 341-17 [16] showed the positive error and it varies from 10% to 95%. The influence of the end connection on the ductility of braced frame needs to be considered for the design and performance evaluation of the SCBFs structures.

Table 7. Comparison of the experimental fracture ductility with AISC 41-17

	Present study			ASCE 41-17			
Specimen	ε_T	ε_C	ε_{Total}	Displacement ductility (T)	Error (%)	Displacement ductility (C)[b]	Error (%)
OOPB	0.0130	0.0172	0.030	9	9.5	7.6	48
IPB	0.0104	0.0116	0.022	9	30	7.6	94
DC	0.0112	0.0098	0.021	9	31	7.0	92

[a] T represent the tension side of the hysteresis cycle.
[b] C represent the compression side of the hysteresis cycle

The post-buckling strength is used in the design of beams and columns of the braced frame system to predict the worst load case scenario. Empirical formula is generally used to calculate the post-buckling strength of the braced system. AISC 341-16 [8] used 30% of the first critical buckling load as the post-buckling load. In the Eurocode 8 [18], the post buckling load is calculated as the 30% of the tensile strength of the brace member. Table 6 shows the post-buckling strength observe in the experiment and compare with that of AISC 341-16 and Eurocode 8. The findings showed that by enhancing the ductility of the brace member, the post buckling strength need to be reevaluated incorporating the influence of the end hinges of the braced frame.

Table 6. Comparing the experimental and various codal post buckling strength

Specimen	Post-Buckling strength			Error	
	Experiemnt $P_{b(\exp)}$ (kN)	AISC-341-16 (kN)	Eurocode 8 (kN)	AISC-341-16 (%)	Eurocode (%)
OOPB	16.32	42.3	58.05	159.2	255.7
IPB	13.76	42.3	58.00	207.4	321.5
DC	38.93	56.73	60.93	45.7	56.5

7. Conclusion and Future work

This paper is focused on the influence of the end hinges on the performance of the various parameter of the SCBFs system. Large-scale tests with three different end connections, namely, OOPB, IPB and DC, were

tested with all other parameters keeping constant. The critical limit states for the three connection were discussed and incorporated in the design to prevent the failure of the end connection.

The conclusions drawn from the experimental study are as follows:

1. The rigidity of the end hinges has strong influence on the overall performance of the braced frame system. OOPB brace system, which provides low stiffness, has shown a better performance than that of IPB and DC brace system.
2. The performance of the DC brace system is comparable to that of IPB system. It is found that in DC braced system, the plastic strain is accumulated at the end hinges of the specimen which enhanced the ductility of the system.
3. All brace specimen showed all the damage states before final fracture at the middle of the brace system. But, the axial strain at which the damage states observed is varied. Specimens with the higher ductility showed the higher axial strain level for a given damage state.
4. The end connection greatly influences the design parameters of the SCBF structures. The displacement ductility proposed by AISC 41-17 is found out to be unconservative for the design and evaluation of the brace system.
5. It is observed that by lowering the stiffness of the end hinges, the post buckling strength also reduces and that need to be considered in the design of the beam and column.
6. The proposed design procedure to prevent premature failure of the critical limit states showed the desire result without any connection failure.

Further research is required to generalize the finding of the present study and incorporate slenderness and compactness ratios to predict the ductility and the post-buckling strengths of braces. The behavior of IPB specimen, which is the most resilient connection, need to be checked for the higher linear clearance for enhancing the performance of the SCBF system.

8. References

[1] D.E. Lehman, C.W. Roeder, D. Herman, S. Johnson, B. Kotulka, Improved seismic performance of gusset plate connections, *J. Struct. Eng.* 134 (2008) 890–901. https://doi.org/10.1061/(ASCE)0733-9445(2008)134:6(890).

[2] R. Tremblay, Inelastic seismic response of steel bracing members, *J. Constr. Steel Res.* 58 (2002) 665–701. https://doi.org/10.1016/S0143-974X(01)00104-3.

[3] P.C.A. Kumar, D.R. Sahoo, N. Kumar, Limiting values of slenderness ratio for circular braces of concentrically braced frames, *J. Constr. Steel Res.* 115 (2015) 223–235. https://doi.org/10.1016/j.jcsr.2015.08.026.

[4] B. V. Fell, A.M. Kanvinde, G.G. Deierlein, A.T. Myers, Experimental investigation of inelastic cyclic buckling and fracture of steel braces, *J. Struct. Eng.* 135 (2009) 19–32. https://doi.org/10.1061/(ASCE)0733-9445(2009)135:1(19).

[5] P.C. Ashwin Kumar, D.R. Sahoo, Fracture ductility of hollow circular and square steel braces under cyclic loading, *Thin-Walled Struct.* 130 (2018) 347–361. https://doi.org/10.1016/j.tws.2018.06.005.

[6] E.J. Lumpkin, Enhanced Seismic Performance of Multi-Story Special Concentrically Brace Frames using a Balanced Design Procedure, *University of Washington*, 2009.

[7] P. Patra, P.C.A. Kumar, D.R. Sahoo, Cyclic Performance of Braces with Different Support Connections in Special Concentrically Braced Frames, *Key Eng. Mater.* 763 (2018) 694–701. https://doi.org/10.4028/www.scientific.net/KEM.763.694.

[8] AISC, Seismic Provisions for Structural Steel Buildings, *ANSI/ AISC 341-10*, Chicago. (2016).

[9] AIJ, Recommendation for Connections in Steel Structures, *Archit. Inst. Japan*, Tokyo. (2012).

[10] C.W. Roeder, E.J. Lumpkin, D.E. Lehman, A balanced design procedure for special concentrically braced frame connections, *J. Constr. Steel Res.* 67 (2011) 1760–1772. https://doi.org/10.1016/j.jcsr.2011.04.016.

[11] P. Patra, D.R. Sahoo, A.K. Jain, Impact of End Protected Zones on Fracture Ductility of Special Concentrically Braced Frame for Ductility-Based Design, *J. Struct. Eng.* (2020) (Submitted).

[12] C.-Y. Tsai, K.-C. Tsai, P.-C. Lin, W.-H. Ao, C.W. Roeder, S.A. Mahin, C.-H. Lin, Y.-J. Yu, K.-J. Wang, A.-C. Wu, J.-C. Chen, T.-H. Lin, Seismic Design and Hybrid Tests of a Full-Scale Three-Story Concentrically Braced Frame Using In-Plane Buckling Braces, *Earthq. Spectra.* 29 (2013) 1043–1067. https://doi.org/10.1193/1.4000165.

[13] A.D. Sen, C.W. Roeder, J.W. Berman, D.E. Lehman, C.-H. Li, A. Wu, K. Tsai, Experimental Investigation of Chevron Concentrically Braced Frames with Yielding Beams, *J. Struct. Eng.* 142 (2016) 04016123. https://doi.org/10.1061/(ASCE)ST.1943-541X.0001597.

[14] P. Patra, D.R. Sahoo, A.K. Jain, Experimental Investigation of Special Concentrically Braced Frames with In-plane Buckling Braces for Ductility-based Design, *12th Can. Conf. Earthq. Eng.* Quebec City, June 17-20. (2019).

[15] K.A. Skalomenos, M. Nakashima, M. Kurata, Seismic capacity quantification of gusset-plate connections to fracture for ductility-based design, *J. Struct. Eng.* 144 (2018) 04018195. https://doi.org/10.1061/(ASCE)ST.1943-541X.0002193.

[16] ASCE, Seismic evaluation and retrofit of existing buildings, *ASCE/SEI 41-17*, Rest. (2017).

[17] S. Evaluation, E. Buildings, Seismic Evaluation and Retrofit of Existing Buildings, Seism. Eval. Retrofit Exist. Build. (2017). https://doi.org/10.1061/9780784414859.

[18] EN 1998–1-1, Eurocode 8: Design of structures for earthquake resistance-part 1: general rules, seismic actions and rules for buildings, CEN, 2005. (2005).

